Continuous Broadband GaAs and GaN MMIC Phase Shifters

Megan Robinson, *Member, IEEE*, Paige Danielson, *Member, IEEE*, and Zoya Popović, *Fellow, IEEE*

Abstract— We describe the design of two broadband monolithic microwave integrated circuit (MMIC) loaded-line reflective phase shifters and their performance over the 6–12-GHz band. Lange couplers with transistor-loaded transmission-line reactive loads provide variable phase shift through reverse-bias control. A GaAs phase shifter with four diode-connected transistors in each of the two reactive loads is designed with discrete inductors to provide an increasing phase shift with frequency. A GaN reflective phase shifter uses 14 transistors in each reactive load with a goal of increasing the phase shift across the band. Measurements show continuous phase shift from 40° to 70° with less than 6-dB insertion loss over the 6–10-GHz band and from 60° to 165° with less than 8-dB insertion loss across the 8–12-GHz band for the GaAs and GaN MMICs, respectively. The power performance of the MMICs is compared in terms of large-signal *S*-parameters, harmonics, and IP3. The GaN phase shifter exhibits similar level of harmonic generation like the GaAs device at a 20-dB higher input power.

Index Terms— Broadband, GaAs, GaN, monolithic microwave integrated circuit (MMIC), phase shifter.

I. INTRODUCTION

PHASE shifters are common components in analog beam-formers of phased array antennas, as well as in instrumentation, e.g., reflectometers or phase-noise discriminators. Phase shifter circuit architectures vary depending on the operational bandwidth and can be digital or continuous [1]. Table I shows a comparison of published continuous broadband ($>40\%$) phase shifters demonstrated in the X-band frequency range, with the two monolithic microwave integrated circuit (MMIC) phase shifters presented in this letter highlighted in bold, where [2] is the best commercially available device in this frequency range. In [3]–[6], the topology is reflective with different hybrids (branch-line, Lange) and variable reflective loads implemented with MEMS [7] or varactors [3], [8]. Large continuous phase shifts in [8]–[10] are accomplished with two cascaded phase shifters. Loaded transmission-line circuits can provide a true time delay over as much as a decade bandwidth shown in discrete phase shifters, e.g., [11]. The loaded-line phase shifters are varied using varactors [12], MEMS [13], or ferroelectrics [14], [15] and are typically limited by return
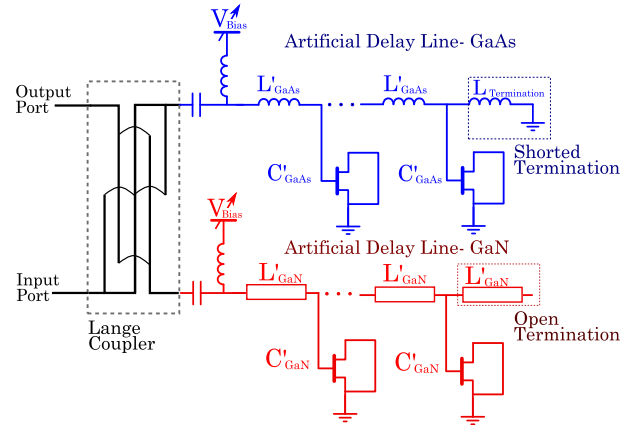
Fig. 1. Topology of reflective loaded-line continuous broadband phase shifter. The coupled and through ports of the Lange coupler are variable reactances, as in a reflective phase shifter. The variable reactances are implemented with tunable artificial transmission lines that use diode-connected transistors as variable capacitors. Both reactive loads are implemented with lumped inductors and a shorted termination in the GaAs MMIC (blue) and with transmission-line sections and an open termination in the GaN MMIC (red).

TABLE I
SUMMARY OF BROADBAND PHASE SHIFTERS AT X-BAND

Ref.	f_c, GHz	FBW, %	$\Delta\Phi$	IL, dB	Topology
[5]	10.2	43	105	3	Reflective
[6]	12	100	120	4	Reflective
[9]	10.25	114	98	9	Reflective dual
[10]	9.75	67	90	3.65	Reflective dual
[15]	10	40	285	11	Loaded Line
[2]	11.5	113	400	8	N/A
GaAs	**8**	**50**	**71**	**6**	**Reflective**
GaN	**10**	**40**	**167**	**7.4**	**Reflective**

loss variation over frequency. This variable characteristic impedance has been addressed by adding additional tunable components, demonstrated at lower frequencies in [16] at 1 GHz and [17] at 5 GHz.

Here, we present broadband GaAs (6–10 GHz) and GaN (8–12 GHz) continuous MMIC phase shifters, with a topology as shown in Fig. 1. To achieve a good match and large phase shift across a broad bandwidth, the circuit in Fig. 1 combines a reflective topology with a loaded-line variable reactance. Two circuits are implemented: a GaAs MMIC with increasing phase in frequency and a GaN MMIC with maximum phase shift in the center of the band. The designs are presented in Section II and the measured results in Sections III and IV, with a comparison of harmonic generation and IP3 dependence on input power. To the best of the authors' knowledge, this is
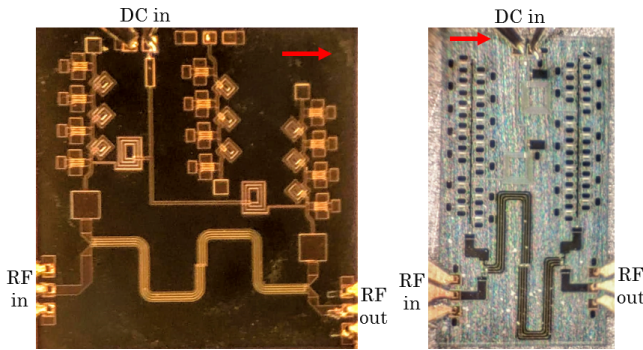
Fig. 2. Photographs of 2.5 mm × 2.5 mm GaAs and 1 mm × 2.5 mm GaN chips. The gate directions for the chips are indicated with red arrows. The effects of bends in the Lange couplers are compensated with electrical length and bridge placement.

the first comparison of broadband GaAs and GaN monolithic phase shifters in terms of power performance.

II. MMIC PHASE SHIFTER CIRCUIT DESIGN

The phase shifters are designed following well-known methods in, e.g., [18] and are implemented in WIN Semiconductors' GaAs enhancement (E-mode) PIH10 and GaN depletion (D-mode) NP15-00 pHEMT processes. Each variable capacitor in Fig. 1 is implemented with a transistor with grounded source and drain terminals. The capacitance range is 0.241–0.470 pF at 9 GHz for gate bias variations of -0.2 to 0.6 V for the GaAs E-mode devices and 0.163–0.281 pF at 9 GHz for -3 to -1-V gate bias variation for the D-mode GaN devices. Fig. 2 shows photographs of the two fabricated MMICs. The GaAs phase shifter uses three lumped 0.4-nH inductors and four transistors in each shorted loaded line. The GaN phase shifter loaded lines are open-circuited and use 14 transistors with electrically short, 95-Ω lines as series inductors. The lines are 15 μm wide and 65 μm long (1.7° at 12 GHz). The periphery of the pHEMTs is chosen to approximately scale with power density of the processes: 4 × 75 μm in GaAs ($\approx$1.5 W/mm) and 2 × 75 μm in GaN ($\approx$3.5 W/mm). The circuits are designed using foundry nonlinear models and full-wave simulations in Cadence AWR.

III. SMALL-SIGNAL MEASUREMENTS

The fabricated chips are measured with a probe station and network analyzer with on-wafer SOLT calibration standards. Fig. 3 shows the measured S-parameter magnitudes from 6 to 12 GHz for the GaAs (blue) and GaN (red) phase shifters, for three gate bias voltages corresponding to the edges and center of the phase range. The dashed lines show the simulated behavior for the same bias conditions. The match remains below 10 dB for both the devices across the range due to the reflective topology. The nonlinear models predict the capacitance changes well, but at slightly different gate voltages than in measurement, resulting in a frequency shift between the measured and simulated data. Depending on the bias and frequency, the transmission amplitude varies and needs to be evaluated together with phase changes.

Fig. 4 shows the measured and simulated phase of S_{21} as a function of control voltage and phase shift and group delay as
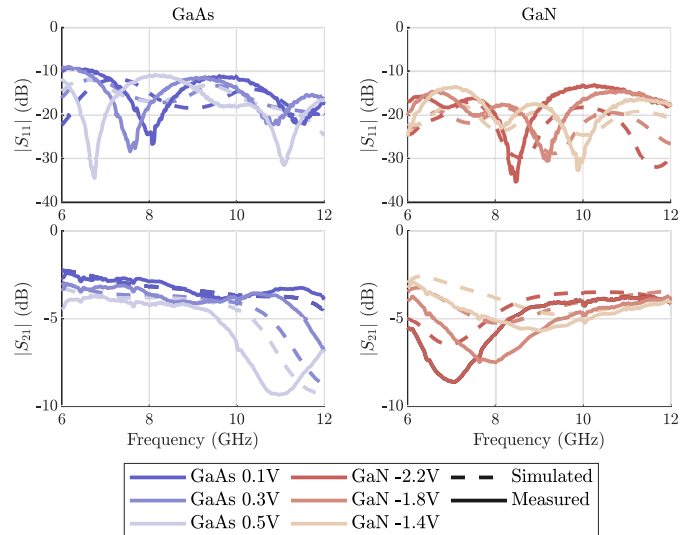

Fig. 3. Simulated and measured S-parameters for both GaAs and GaN chips at three bias voltages of interest.
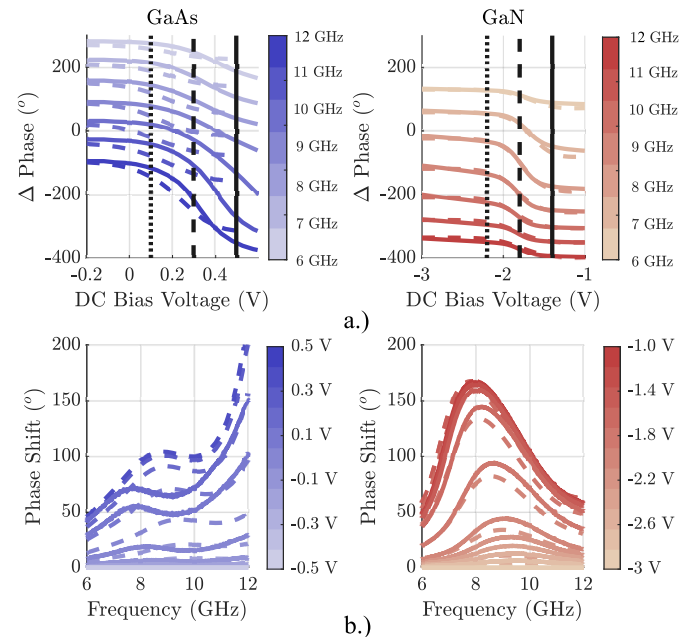

Fig. 4. (a) Measured and simulated phase as a function of gate bias. The black lines indicate lower (fine dashed), middle (dashed), and upper (solid) biases for a useful voltage range. For this range, (b) shows the measured and simulated phase variation for 6–12 GHz. The results for the GaAs and GaN MMICs are shown on the left (blue) and right (red), respectively.

a function of frequency. The useful voltage range is indicated with vertical black lines in Fig. 4(a) for both MMICs. For this range, the phase is plotted across frequency in Fig. 4(b), showing that with appropriate choice of bias control, the GaAs and GaN MMICs have 40°–150° and 60°–165° of phase variation, respectively. Ideally, for artificial transmission lines, the group delay should be flat, but the reflective topology adds additional dispersion.

The reactive line in the GaAs MMIC is electrically shorter and the phase shifter has more phase variation at the higher frequency, which is useful for broadband phased array feed networks. On the other hand, the reactive line in the GaN phase shifter is electrically long and supports an in-band resonance.
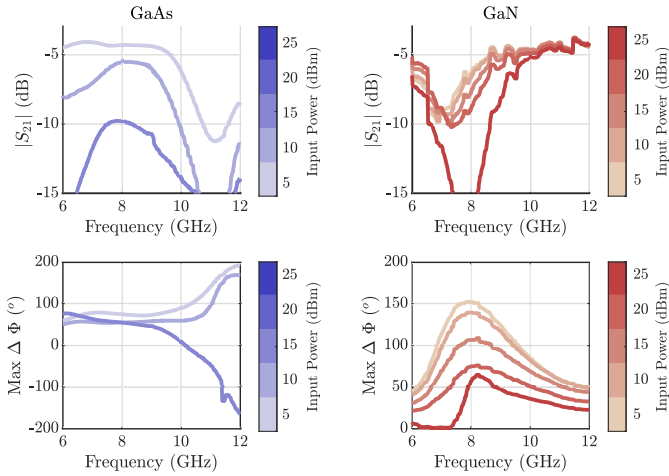
Fig. 5. Measured frequency dependence of transmission coefficient (top) and maximum phase shift (bottom) for an input power range of 5–25 dBm in steps of 5 dB. $|S_{21}|$ is plotted at the highest voltage for the GaAs (left, blue) and GaN (right, red) devices. The GaAs circuit is too lossy above $P_{in} = 15$ dBm.

The phase shift peaks around 8 GHz and is 20° higher at the lower edge of the band and 90° lower at the higher edge of the band, compared with the GaAs phase shifter.

IV. LARGE-SIGNAL NONLINEAR PERFORMANCE

Large-signal measurements are performed with a network analyzer calibrated with a linear amplifier at the input port. Fig. 5 shows the amplitude and phase change of the large-signal transmission coefficient. A frequency-dependent increase in loss and a reduction in phase change are observed for both MMICs, but at different power levels, as expected. For the GaAs MMIC, above 10 dBm of input power, the device provides 50°–60° of phase shift but $|S_{21}|$, drops below −15 dB. On the other hand, the GaN MMIC has 20°–75° of phase shift for up to 20 dBm of input power with little variation in $|S_{21}|$ compared with the small-signal case. The power dependence eventually levels, because the first diode behaves as a short and the phase is no longer tunable. The GaN phase shifter has higher power handling since the transistor gate–source breakdown voltage exceeds 100 V and is limited by the gold 95-Ω transmission line to about 7 W, by the manufacturer.

To quantify the harmonics, a CW signal is amplified with a linear amplifier and the output harmonic content measured with a spectrum analyzer. A coupler and power meter at the chip input enable calibrated power measurements. The results are shown in Fig. 6. The harmonic generation is frequency- and bias-dependent for both MMICs. The GaN phase shifter generates the same harmonic level at a 20-dB higher input power than the GaAs circuit, as expected.

Two-tone measurements with 5, 10, and 15 MHz tone spacings are performed with two identical CW sources and a broadband power combiner followed by a linear amplifier, with power measured at the output of the MMICs with a spectrum analyzer. The results are shown in Fig. 7. Note that the bias has a greater effect than in the case of CW measurements, and that the third-order intermodulation products (IP3) are significantly
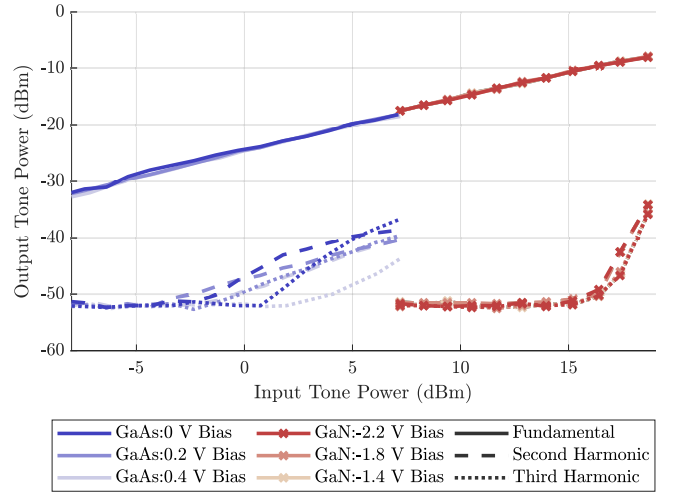

Fig. 6. Harmonic generation as a function of input power for the GaAs (blue) and GaN (red) phase shifters at 9 GHz.
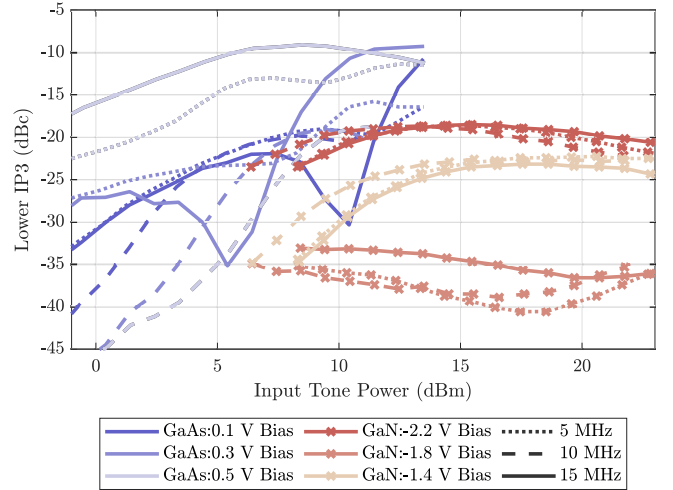

Fig. 7. Lower IP3 tone as a function of input tone power measured at 9 GHz for tone spacings of 5, 10, and 15 MHz, at three bias voltages for the GaAs (blue) and GaN (red) circuits.

higher in level than the harmonics. The GaN MMIC does not show further increase in IP3 after 15 dBm.

V. CONCLUSION

This letter compares GaAs and GaN broadband MMIC phase shifters with a combined reflective and loaded-line topology. The GaN MMIC tolerates higher input powers, which is not surprising, but is quantified here for the first time. For the same harmonic content generation and IMD3 levels, the GaN MMIC requires 20 dBm higher input power, while the phase and amplitude degrade at 15 dBm higher power.

REFERENCES

[1] S. K. Koul and B. Bhat, *Microwave and Millimeter Wave Phase Shifters*, vol. 2. Norwood, MA, USA: Artech House, 1991.

[2] *Analog Phase Shifters, HMC247 Datasheet*, Analog Devices, Norwood, MA, USA, 2021.

[3] J. J. P. Venter, T. Stander, and P. Ferrari, "X-band reflection-type phase shifters using coupled-line couplers on single-layer RF PCB," *IEEE Microw. Wireless Compon. Lett.*, vol. 28, no. 9, pp. 807–809, Sep. 2018.

[4] A. N. Sychev, I. M. Dobush, N. Y. Rudyi, and S. M. Struchkov, "Analog phase shifter of X-band implemented with novel trans-directional coupled-line coupler," in *Proc. 48th Eur. Microw. Conf. (EuMC)*, Sep. 2018, pp. 811–814.

[5] O. Dawson, A. Conti, S. Lee, G. Shade, and L. Dickens, "An analog X-band phase shifter," in *Proc. Microw. Millim.-Wave Monolithic Circuits*, May/Jun. 1983, vol. 84, no. 1, pp. 6–10.

[6] D. M. Krafcsik, S. A. Imhoff, D. E. Dawson, and A. L. Conti, "A dual-varactor analog phase shifter operating at 6 to 18 GHz," *IEEE Trans. Microw. Theory Techn.*, vol. 36, no. 12, pp. 1938–1941, Dec. 1988.

[7] G. M. Rebeiz, G.-L. Tan, and J. S. Hayden, "RF MEMS phase shifters: Design and applications," *IEEE Microw. Mag.*, vol. 3, no. 2, pp. 72–81, Jun. 2002.

[8] W.-T. Li, Y.-H. Kuo, Y.-M. Wu, J.-H. Cheng, T.-W. Huang, and J.-H. Tsai, "An X-band full-360° reflection type phase shifter with low insertion loss," in *Proc. 7th Eur. Microw. Integr. Circuit Conf.*, Oct. 2012, pp. 754–757.

[9] S. Lucyszyn and I. D. Robertson, "Two-octave bandwidth monolithic analog phase shifter," *IEEE Microw. Guided Wave Lett.*, vol. 2, no. 8, pp. 343–345, Aug. 1992.

[10] S. Lucyszyn and I. D. Robertson, "High performance octave bandwidth MMIC analogue phase shifter," in *Proc. 22nd Eur. Microw. Conf.*, vol. 1, Sep. 1992, pp. 221–224.

[11] N. S. Barker and G. M. Rebeiz, "Distributed MEMS true-time delay phase shifters and wide-band switches," *IEEE Trans. Microw. Theory Techn.*, vol. 46, no. 11, pp. 1881–1890, Nov. 1998.

[12] X. Sun, J.-M. Fernandez-Gonzalez, M. Sierra-Perez, and B. Galocha-Iraguen, "Low-loss loaded line phase shifter for radar application in X band," in *Proc. 15th Eur. Radar Conf. (EuRAD)*, Sep. 2018, pp. 477–480.

[13] J. S. Hayden and G. M. Rebeiz, "Low-loss cascadable MEMS distributed X-band phase shifters," *IEEE Microw. Guided Wave Lett.*, vol. 10, no. 4, pp. 142–144, Apr. 2000.

[14] M. Sazegar, Y. Zheng, H. Maune, X. Zhou, C. Damm, and R. Jakoby, "Compact artificial line phase shifter on ferroelectric thick-film ceramics," in *IEEE MTT-S Int. Microw. Symp. Dig.*, May 2010, pp. 860–863.

[15] D. Mercier *et al.*, "X band distributed phase shifter based on sol-gel BCTZ varactors," in *Proc. Eur. Radar Conf. (EURAD)*, Oct. 2017, pp. 382–385.

[16] F. Lin and H. Deng, "Continuously tunable true-time-delay phase shifter based on transmission lines with simultaneously reconfigurable impedance and phase constant," *IEEE Trans. Microw. Theory Techn.*, vol. 67, no. 12, pp. 4714–4723, Dec. 2019.

[17] C. Damm, M. Schubler, J. Freese, and R. Jakoby, "Artificial line phase shifter with separately tunable phase and line impedance," in *Proc. Eur. Microw. Conf.*, Sep. 2006, pp. 423–426.

[18] S. K. Koul and B. Bhat, *Microwave and Millimeter Wave Phase Shifters*. Norwood, MA, USA: Artech House, 1991.